



**HAL**  
open science

## Semi-volatile organic compounds in French dwellings An estimation of concentrations in the gas phase and particulate phase from settled dust

Wenjuan Wei, Corinne Mandin, Olivier Blanchard, F. Mercier, M. Pelletier, Barbara Le Bot, Philippe Glorennec, Olivier Ramalho

### ► To cite this version:

Wenjuan Wei, Corinne Mandin, Olivier Blanchard, F. Mercier, M. Pelletier, et al.. Semi-volatile organic compounds in French dwellings An estimation of concentrations in the gas phase and particulate phase from settled dust. *Science of the Total Environment*, 2019, 650, pp.2742-2750. 10.1016/j.scitotenv.2018.09.398 . hal-01904740

**HAL Id: hal-01904740**

**<https://univ-rennes.hal.science/hal-01904740>**

Submitted on 9 Nov 2018

**HAL** is a multi-disciplinary open access archive for the deposit and dissemination of scientific research documents, whether they are published or not. The documents may come from teaching and research institutions in France or abroad, or from public or private research centers.

L'archive ouverte pluridisciplinaire **HAL**, est destinée au dépôt et à la diffusion de documents scientifiques de niveau recherche, publiés ou non, émanant des établissements d'enseignement et de recherche français ou étrangers, des laboratoires publics ou privés.

# Semi-volatile organic compounds in French dwellings: an estimation of concentrations in the gas phase and particulate phase from settled dust

Wenjuan Wei<sup>1,\*</sup>, Corinne Mandin<sup>1</sup>, Olivier Blanchard<sup>2</sup>, Fabien Mercier<sup>2</sup>, Maud Pelletier<sup>2</sup>,  
Barbara Le Bot<sup>2</sup>, Philippe Glorennec<sup>2</sup>, Olivier Ramalho<sup>1</sup>

<sup>1</sup>University of Paris-Est, Scientific and Technical Center for Building (CSTB), Health and Comfort Department, French Indoor Air Quality Observatory (OQAI), 84 Avenue Jean Jaurès, Champs sur Marne, 77447 Marne la Vallée Cedex 2, France

<sup>2</sup>Univ Rennes, EHESP, Inserm, Irset (Institut de recherche en santé, environnement et travail) - UMR\_S 1085, F-35000 Rennes, France

\*Corresponding author: Centre Scientifique et Technique du Bâtiment (CSTB), Direction Santé-Confort - Observatoire de la Qualité de l'Air Intérieur (OQAI), 84 Avenue Jean Jaurès, Champs sur Marne, 77447 Marne la Vallée Cedex 2, France. Tel.: +331 6468 8457; fax: +331 6468 8823.  
Email address: Wenjuan.Wei@cstb.fr

**ABSTRACT**

Semi-volatile organic compounds (SVOCs) are present in the gas phase, particulate phase and settled dust in the indoor environment, resulting in human exposure through different pathways. Sometimes, SVOCs are only measured in a single phase because of practical and/or financial constraints. A probabilistic method proposed by Wei et al. for the prediction of the SVOC concentration in the gas phase from the SVOC concentration in the particulate phase was extended to model the equilibrium SVOC concentrations in both the gas and particulate phases from the SVOC concentration measured in settled dust. This approach, based on the theory of SVOC partitioning among the gas phase, particulate phase, and settled dust incorporating Monte Carlo simulation, was validated using measured data from the literature and applied to the prediction of the concentrations of 48 SVOCs in both the gas and particulate phases in 3.6 million French dwellings where at least one child aged 6 months to 6 years lived. The median gas-phase concentration of 15 SVOCs, i.e., 5 phthalates, 2 organochlorine pesticides, 4 polycyclic aromatic hydrocarbons (PAHs), 2 synthetic musks, dichlorvos, and tributyl phosphate, was found to be higher than  $1 \text{ ng/m}^3$ . The median concentration of 5 phthalates in the particulate phase was higher than  $1 \text{ ng/m}^3$ . The impacts of some physical parameters, such as the molar mass and boiling point, on the SVOC partitioning among the different phases were quantified. The partitioning depends on the activity coefficient, vapor pressure at the boiling point, entropy of evaporation of the SVOCs, and the fraction of organic matter in particles. Thus, the partitioning may differ from one chemical family to another. The empirical equations based on regressions allow quick estimation of SVOC partitioning among the gas phase, particulate phase, and settled dust from the molar mass and boiling point.

**KEYWORDS**

Partitioning, SVOC, exposure, indoor air quality, settled dust

**1. INTRODUCTION**

Indoor semi-volatile organic compounds (SVOCs) are present in the gas phase, particulate phase and settled dust (Blanchard et al., 2014). The SVOCs in these different phases contribute to human exposure through different pathways, e.g., inhalation, ingestion and dermal exposure (Bekö et al., 2013; Pelletier et al., 2017). SVOCs are sometimes measured in only a single phase, e.g., in a French nationwide survey, the concentrations of 48 SVOCs were measured in settled dust sampled from 145 dwellings located all over France (Mandin et al., 2013). Thus, to assess human exposure, the SVOC concentrations in the other phases need to be estimated from the concentration in the measured phase according to SVOC partitioning theory (Weschler and Nazaroff, 2008).

Pankow proposed a model addressing the equilibrium partitioning of SVOCs between the gas and particulate phases (Pankow, 1994). This model was based on the SVOC partitioning theory characterized by the SVOC particle/gas partition coefficient, which was calculated from the saturation vapor pressure ( $p_L^0$ ) of the SVOCs. Weschler and Nazaroff proposed two equations to address the equilibrium partitioning of SVOCs among the gas phase, particulate phase, and settled dust (Weschler and Nazaroff, 2010). The particle/gas and dust/gas partition coefficients ( $K_p$  and  $K_d$ ) of SVOCs were calculated from the SVOC octanol/air partition coefficients ( $K_{oa}$ ). Moreover, Takeuchi et al. studied the concentrations of 34 SVOCs in the gas and particulate phases in 6

houses in Japan and observed an impact of the SVOC molar mass on the partitioning of SVOCs between the gas and particulate phases (Takeuchi et al., 2014).

Based on SVOC partitioning theory, Wei et al. proposed a probabilistic approach to predict the distribution of the equilibrium SVOC concentrations in the gas phase from the concentrations in the particulate phase while considering the uncertainty in the input parameters (Wei et al., 2017a). This probabilistic approach using Monte Carlo simulation considers the distribution of  $K_p$  and  $K_d$  from  $K_{oa}$  and  $p_L^0$  for each SVOC and the influence of temperature on  $K_p$  and  $K_d$ . This approach was applied to estimate the concentrations of 66 SVOCs in the gas phase in French dwellings from their 1-week average concentrations in the particulate phase. The study concluded that the probabilistic approach is robust and timesaving for the prediction of a large dataset of indoor SVOC concentrations.

The objectives of the present study were (1) to extend the probabilistic approach to the estimation of SVOC concentrations in the gas and particulate phases in French dwellings at a nationwide scale from their measured concentrations in settled dust and (2) to study the influence of the physical parameters of SVOCs, such as the molar mass, boiling point,  $K_{oa}$ , and  $p_L^0$ , on the SVOC partitioning among the gas phase, airborne particles and settled dust.

## 2. MATERIALS AND METHODS

### 2.1. SVOC partitioning theory

The equilibrium partitioning of SVOCs among the gas phase ( $C_g$ ), particulate phase ( $F$ ) and settled dust ( $C_d$ ) in the indoor environment can be characterized as follows (Weschler and Nazaroff, 2010).

$$C_g = \frac{F}{TSP \times K_p} \quad (1)$$

$$C_g = \frac{C_d}{K_d} \quad (2)$$

where  $TSP$  ( $\mu\text{g}/\text{m}^3$ ) is the concentration of the total suspended airborne particles;  $K_p$  and  $K_d$  have units of  $\text{m}^3/\mu\text{g}$  and  $\text{m}^3/\text{g}$ , respectively; and  $C_g$ ,  $F$  and  $C_d$  have units of  $\mu\text{g}/\text{m}^3$ ,  $\mu\text{g}/\text{m}^3$  and  $\mu\text{g}/\text{g}$ , respectively. Combining Eqs. (1) and (2), the relationship between  $F$  and  $C_d$  becomes

$$F = \frac{C_d \times TSP \times K_p}{K_d} \quad (3)$$

Therefore,  $C_g$  and  $F$  can be predicted at equilibrium from  $C_d$  using Eqs. (2) and (3), respectively. A probabilistic method proposed by Wei et al. was originally applied to predict  $C_g$  from  $F$  using Eq. (1) (Wei et al., 2017a). This method, which is suitable for predicting the distribution of  $C_g$  for a large dataset under the assumption of the equilibrium partitioning of SVOCs among different phases, uses Monte Carlo simulation to account for uncertainty in the physical input parameters. To calculate  $C_g$ ,  $F$  and  $TSP$  were retrieved from 1-week integrated measurements in dwellings (Mandin et al., 2016) at conditions assumed to be close to equilibrium, and the distribution of  $K_p$  for a given SVOC was determined from a number of estimates (Wei et al., 2016a). The influence

of the indoor temperature on the distribution of  $K_p$  was taken into account in the calculation (Wei et al., 2016b). This method was extended in the present study to predict  $C_g$  and  $F$  from  $C_d$ . The parameters, i.e.,  $C_d$ ,  $K_p$ ,  $K_d$ , and  $TSP$ , for the prediction are described in detail as follows.

## 2.2. SVOC concentrations in the settled dust of French dwellings

Mandin et al. measured the concentration  $C_d$  of 48 SVOCs in the settled dust of French dwellings (Mandin et al., 2013). Dust samples were collected from 145 dwellings located all over France from October 2008 to August 2009. The dust sample for each dwelling was collected from the household vacuum cleaner bag, which is a mixture of the settled dust from different parts of the dwelling. Therefore, the measured  $C_d$  is the average concentration in the dwelling. The dwellings were randomly selected to constitute a representative sample of dwellings where at least one child aged 6 months to 6 years lived. The 48 SVOCs measured in the settled house dust included organochlorine pesticides (n=7), organophosphorus pesticides (n=3), pyrethroids (n=4), polychlorinated biphenyls (PCBs, n=10), phthalates (n=6), polybrominated diphenyl ethers (PBDEs, n=9), synthetic musks (n=2), polycyclic aromatic hydrocarbons (PAHs, n=5), bisphenol A, and tributyl phosphate.

## 2.3. Distributions of $K_p$ and $K_d$ and the influence of temperature

$K_p$  and  $K_d$  were calculated from  $p_L^0$  and/or  $K_{oa}$ . To avoid bias in the calculated  $K_p$  and  $K_d$ , Wei et al. proposed the calculation of the distributions of  $K_p$  and  $K_d$  using 38 different equations retrieved from the literature (Wei et al., 2016a). These equations generally considered 25 °C as the reference

temperature. The distributions of  $K_p$  and  $K_d$  for 72 SVOCs, including the 48 SVOCs in the present study, were presented in detail elsewhere (Wei et al., 2016a).

The indoor temperature impacts  $K_p$  and  $K_d$ , thereby influencing the partitioning of SVOCs among the different phases. The relationship between  $K_p$  and the indoor temperature is described as follows (Wei et al., 2016b).

$$\log_{10} K_{p2} = \frac{\Delta H}{2.303R} \left( \frac{1}{T_2} - \frac{1}{T_1} \right) + \log_{10} \frac{T_2}{T_1} + \log_{10} K_{p1} \quad (4)$$

where  $T_1$  and  $T_2$  are the reference (298.15 K) and indoor (K) temperatures, respectively;  $K_{p1}$  and  $K_{p2}$  are the particle/gas partition coefficients at the reference and indoor temperatures, respectively;  $R$  (8.314 J/(mol K)) is the ideal gas constant; and  $\Delta H$  (J/mol) is the phase-change enthalpy of evaporation for the SVOCs. This equation was originally developed to address the relationship between the indoor temperature and  $K_p$  and is assumed to be applicable to the relationship between the indoor temperature and  $K_d$  for the present study because airborne particles and settled dust can exchange mass via both deposition and resuspension (Shi and Zhao, 2012).

The indoor temperature was not measured in the 145 French dwellings where the  $C_d$  of the 48 SVOCs was measured. However, indoor temperatures were available from 567 randomly selected French dwellings (Langer et al., 2016). These measurements were carried out continuously over the course of seven days in each dwelling, both in the living room and bedroom. The weekly average temperature in both rooms was calculated. The distribution of the indoor temperature in the French dwellings was determined using XLSTAT 2014 software (Addinsoft, Paris, France) in the present study. The arithmetic mean ( $\pm$ standard deviation) and median 1-week average indoor temperatures in the French dwellings was (20.9 $\pm$ 2.45) °C and 20.8 °C, respectively, with a

maximum of 29.3 °C and a minimum of 13.1 °C. The indoor temperatures could be fitted into a normal distribution (Fig. S1 in the supporting information). The  $p$ -value of the Kolmogorov-Smirnov test of the measured and fitted values was 0.46, indicating that the difference between the measured and fitted values was not significant.

#### **2.4. TSP concentration in the French dwellings**

The *TSP* concentration was not measured in the 145 dwellings where the settled dust concentrations of the 48 SVOCs were measured. However, the indoor  $PM_{10}$  concentration was obtained in 285 randomly selected French dwellings (Brown et al., 2015). The distribution of the measured indoor  $PM_{10}$  concentrations was determined using XLSTAT 2014 software and was assumed to be the distribution of *TSP* for the present study. The arithmetic mean ( $\pm$  standard deviation) and median  $PM_{10}$  concentration in the French dwellings was  $(54\pm 65) \mu\text{g}/\text{m}^3$  and  $31 \mu\text{g}/\text{m}^3$  respectively, with a maximum of  $553 \mu\text{g}/\text{m}^3$  and a minimum of  $1.6 \mu\text{g}/\text{m}^3$ . The indoor  $PM_{10}$  concentration differed largely from one dwelling to another because of occupants' activities, such as smoking. The indoor  $PM_{10}$  concentrations could be fitted to a log-normal distribution (Fig. S2 in the supporting information). The  $p$ -value of the Kolmogorov-Smirnov test of the measured and fitted values was below 0.05 (0.004). This result was mainly explained by the use of  $PM_{10}$  concentrations from some smoker dwellings that were largely higher than those from nonsmoker dwellings.

#### **2.5. Monte Carlo simulation**

Crystal Ball software (Oracle, Redwood Shores, CA, USA) was used to perform the Monte Carlo simulation. The prediction of  $C_g$  and  $F$  from  $C_d$  was carried out using the following parameters and steps. First, for each SVOC, the measured  $C_d$  values in the 145 dwellings (Mandin et al., 2013) were used as inputs.  $C_d$  values below the limit of detection (LOD) were assumed to be uniformly distributed between 0 and the LOD. Second, the simulation of  $C_g$  and  $F$  for each SVOC in each of the 145 dwellings was carried out with  $10^5$  runs using Eqs. (2) and (3), and the distributions of the indoor temperature,  $PM_{10}$  concentration (assumed to be equal to  $TSP$ ), and  $K_p$  and  $K_d$  of each SVOC at 25 °C. For each run, the distributions of  $K_p$  and  $K_d$  were adapted to the estimated indoor temperature using Eq. (4). For each dwelling, the simulation provided distributions of  $C_g$  and  $F$  as outputs. Finally, a sampling weight was assigned to each of the 145 dwellings to represent the 3.6 million dwellings in France where at least one child aged 6 months to 6 years lived. The sampling weight, presented in detail elsewhere (Mandin et al., 2013), was introduced to obtain the weighted distributions of  $C_g$  and  $F$  within the 3.6 million dwellings using XLSTAT software.

## 2.6. Validation of the method

To validate this method, it was applied to two studies available in the literature with simultaneous raw data measurements of  $C_g$ ,  $F$  and  $C_d$ . The predicted  $C_g$  and  $F$  values from the measured  $C_d$  were compared with the measured  $C_g$  and  $F$ . The first study measured phthalates, PCBs, pesticides, PAHs and tributyl phosphate in 30 living and family rooms in France (Blanchard et al., 2014). The second study measured PBDEs in 12 rooms in homes in the U.S. (Batterman et al., 2009).

Crystal Ball software was used to perform the Monte Carlo simulation. The input parameters were defined as follows. For each SVOC, the measured  $C_d$  in each room was input into the software.

The *TSP* concentrations were not provided in the two studies used for validation. Therefore, the median one-week  $PM_{10}$  concentration ( $31 \mu\text{g}/\text{m}^3$ ) measured in 285 French dwellings (Brown et al., 2015) was assumed to be a reasonable estimate of the *TSP* concentration in the 12 U.S. rooms. The median  $PM_{10}$  concentration in nonsmoker ( $26 \mu\text{g}/\text{m}^3$ ) and smoker ( $63 \mu\text{g}/\text{m}^3$ ) dwellings (Langer et al., 2016) was assumed to be a reasonable estimate of the *TSP* concentration for the French study (27 nonsmoker rooms and 3 smoker rooms). The indoor temperature, which ranged between  $16.6 \text{ }^\circ\text{C}$  and  $22.7 \text{ }^\circ\text{C}$ , was measured in each of the 30 French rooms. In the U.S. study, an indoor temperature of  $25 \text{ }^\circ\text{C}$  was measured in some U.S. rooms and assumed to be the same in the other environments. Monte Carlo simulation of the  $C_g$  and  $F$  of each SVOC in each room provided a distribution from which the median  $C_g$  and  $F$  were retrieved for comparison with the measured values. The determination coefficients ( $R^2$ ) and relative biases between the measured and predicted values were analyzed quantitatively. A comparison was conducted for chemicals with measured values in each room that were above the limit of quantification (LOQ) in the French study and above the LOD in the U.S. study.

### 3. RESULTS AND DISCUSSION

#### 3.1. Validation of the method for 23 SVOCs

To validate the method in the present study, the predicted and measured  $C_g$  and  $F$  values were compared for 7 PBDEs (Batterman et al., 2009), 2 PAHs, 6 phthalates, 3 pesticides, 4 PCBs and tributyl phosphate (Blanchard et al., 2014). For some PCBs, diazinon, and dieldrin, the predicted and observed values could be compared only in a single room for which the measurements within each room were above the LOQ. For the other 17 SVOCs, the values could be compared in at least

2 rooms. The predicted median values for all SVOCs in all rooms were in reasonable agreement with the measured values (Fig. 1). The  $R^2$  values between the predictions and measurements were 0.96 and 0.92 for  $C_g$  and  $F$ , respectively. At the room level, the predicted and measured  $C_g$  and  $F$  varied by one order of magnitude, depending on the SVOC (Fig. S3 in the supporting information). The corresponding  $R^2$  values varied between 0.02 (tributyl phosphate) and 0.99 (dieldrin) for  $C_g$  and between 0.02 (phenanthrene) and 0.94 (BDE 154) for  $F$  (Table S1 in the supporting information). On average, the relative bias, defined as the difference between the predicted and measured values divided by the measured value, ranged from 5% (BBP) to 225% ( $\gamma$ -HCH) for  $C_g$  and between 2% (BDE 153) and 249% (DiNP) for  $F$ , considering the absolute values. The bias in the prediction at the room level may be explained by the assumption that all the rooms had the same indoor temperature and  $TSP$ . Moreover, the equilibrium partitioning of SVOCs may not have been reached in all the rooms for all the compounds. Some recent studies have shown that equilibrium partitioning is unlikely to be reached in indoor environments when the  $\log_{10}K_{oa}$  value is  $>11$  for PCBs (Zhang et al., 2011),  $>12$  for organophosphate ester flame retardants (Vykoukalová et al., 2017), and  $>14$  for brominated flame retardants (Venier et al., 2016). Despite the bias in the predictions at the room level for the 17 SVOCs, this comparison showed that the probabilistic approach described in the present study can provide reasonable estimates of the median  $C_g$  and  $F$  values from a dataset of  $C_d$ .

Fig. 1. Comparison between the predictions and measurements

### 3.2. Concentrations of SVOCs in the air of French dwellings

The distributions of  $C_g$  and  $F$  of the 48 SVOCs were predicted from  $C_d$  at a nationwide scale in France. The shapes of the distributions depend on the compound and do not have a regular pattern. An example of DEHP and DBP is shown in Fig. 2. The ranges of the median  $C_g$  and  $F$  of the 48 SVOCs (in 8 categories) are shown in Fig. 3. The  $C_g$  and  $F$  of phthalates and PAHs were higher than those of PBDEs and PCBs. Fifteen SVOCs had a median  $C_g$  that was higher than  $1 \text{ ng/m}^3$ , i.e., di(2-ethylhexyl) phthalate (DEHP,  $2.7 \text{ ng/m}^3$ ), diethyl phthalate (DEP,  $320 \text{ ng/m}^3$ ), diisobutyl phthalate (DiBP,  $270 \text{ ng/m}^3$ ), di-n-butyl phthalate (DBP,  $97 \text{ ng/m}^3$ ), butyl benzyl phthalate (BBP,  $7.8 \text{ ng/m}^3$ ), dichlorvos ( $40 \text{ ng/m}^3$ ),  $\gamma$ -hexachlorocyclohexane ( $\gamma$ -HCH,  $2.4 \text{ ng/m}^3$ ),  $\alpha$ -endosulfan ( $1 \text{ ng/m}^3$ ), phenanthrene ( $94 \text{ ng/m}^3$ ), fluorene ( $66 \text{ ng/m}^3$ ), acenaphthene ( $35 \text{ ng/m}^3$ ), anthracene ( $18 \text{ ng/m}^3$ ), galaxolide ( $32 \text{ ng/m}^3$ ), tonalide ( $8.4 \text{ ng/m}^3$ ) and tributyl phosphate ( $21 \text{ ng/m}^3$ ). Five SVOCs had a median  $F$  that was higher than  $1 \text{ ng/m}^3$ , i.e., DEHP ( $5.7 \text{ ng/m}^3$ ), DiBP ( $3.3 \text{ ng/m}^3$ ), DBP ( $3.3 \text{ ng/m}^3$ ), DEP ( $2.2 \text{ ng/m}^3$ ), and BBP ( $1.3 \text{ ng/m}^3$ ) (Table 1). Six of the 48 SVOCs, i.e., BDE 209, BDE 154, BDE 153, bisphenol A, DEHP, and DiNP, have  $\log_{10}K_{oa}$  values  $>12$  (Fig. S4 in the supporting information). The equilibrium partitioning of these SVOCs between the airborne phases and settled dust may not have been reached. Therefore, the predictions of the present model for these SVOCs may be less precise than those for the other SVOCs having  $\log_{10}K_{oa}$  values  $<12$ .

Fig. 2. Distributions of the predicted gas and particle-phase concentrations of DEHP and DBP
--

Fig. 3. Ranges of the median $C_g$ and $F$ of 48 SVOCs in French dwellings
--

Table 1. SVOC concentrations in the gas phase ( $C_g$ ) and airborne particles ( $F$ )
--

The  $F$  predicted in the present study from the  $C_d$  measured between 2008 and 2009 (Mandin et al., 2013) was compared with the  $F$  measured (PM<sub>10</sub> fraction) between 2003 and 2005 (Mandin et al., 2016). The median values of  $F$  in the two studies generally varied within one order of magnitude

(Fig. 4). The two independent studies suggest similar levels of SVOC concentrations in French dwellings. Differences of more than one order of magnitude were observed for DiNP, PCB 28, PCB 31, PCB 52,  $\alpha$ -endosulfan, diazinon, anthracene, phenanthrene, and bisphenol A. The difference in  $F$  between the two studies may be because the dwellings selected in the two studies were different and were sampled at two different periods. Nevertheless, for DiNP and bisphenol A ( $\log_{10}K_{oa}$  values  $>12$ ), equilibrium partitioning between the particle phase and settled dust may not have been reached. It can also be a reason for the uncertainties in the predictions.

The  $C_g$  predicted in the present study from the  $C_d$  measured between 2008 and 2009 (Mandin et al., 2013) was compared with the  $C_g$  (Wei et al., 2017a) predicted from  $F$  measured between 2003 and 2005 (Mandin et al., 2016). The median  $C_g$  in the two studies generally varied within one order of magnitude (Fig. 5). Differences of more than one order of magnitude were observed for DEHP, DiNP, PCB 28,  $\alpha$ -endosulfan, diazinon, anthracene, phenanthrene, and bisphenol A. For DEHP, DiNP and bisphenol A ( $\log_{10}K_{oa}$  values  $>12$ ), equilibrium partitioning between the gas phase and settled dust may not have been reached. For the other SVOCs, the concentration difference between the two studies may be explained by the difference in the sampling locations and periods.

Fig. 4. Comparison between the measured and predicted SVOC concentrations in the particulate phase (error bars represent the 1<sup>st</sup> and 3<sup>rd</sup> quartiles of the concentrations)

Fig. 5. Comparison between the predicted SVOC concentrations in the gas phase (error bars represent the 1<sup>st</sup> and 3<sup>rd</sup> quartiles of the concentrations)

SVOC mass transfer mechanisms have been investigated in depth in a number of studies (Liu et al., 2012; Rauert and Harrad, 2015; Takigami et al., 2008; Webster et al., 2009; Weschler and Nazaroff, 2017; Wu et al., 2018; Xu et al., 2012). Mechanistic models that do not rely on the equilibrium partitioning assumption have been developed to address the dynamic SVOC mass transfer processes (Wei et al., 2017b; Xu et al., 2010). The present study did not choose an in-depth mechanistic model for the prediction because these models usually require detailed information on indoor environments and a number of mass transfer parameters as inputs. Although these parameters can be obtained for case studies, they are unlikely to be retrievable for a study of a large dataset of dwellings, e.g., a prediction at a nationwide scale in France in the present study. Therefore, the present study chose the equilibrium partitioning equations and extended them into a probabilistic method using Monte Carlo simulation and taking into account the indoor temperature. The probabilistic method aims to provide robust and efficient predictions for a large dataset of indoor environments and is not intended for use in a specific room. At the room level, this method may be less precise than an in-depth mechanistic model.

Moreover, some outdoor studies show that SVOC polarity has an influence on the  $K_p$  and  $K_d$  values (Lohmann and Lammel, 2004). The relationship between  $K_p$  and polarity was quantified by an empirical equation based on measurements (Degrendele et al., 2016), suggesting that for a pesticide with a  $\log_{10}K_{oa}$  value of 10 at 25 °C, the polarity can affect the  $\log_{10}K_p$  value by 7%. However, there has not been any study to quantify the influence of the SVOC polarity on the  $K_p$  and  $K_d$  values for indoor airborne particles and settled dust. The 38 equations retrieved from the literature for the probabilistic prediction calculate the indoor  $K_p$  and  $K_d$  from  $p_L^0$  and/or  $K_{oa}$  (Wei et al., 2016a) and do not have any item to address polarity. This may lead to some errors in the prediction of polar compounds. Among the 48 SVOCs studied in the French nationwide survey,

the top 10 SVOCs in terms of molecular polarity (indicated by dipole moment) are tributylphosphate (5.5 D), cypermethrin (4.2 D), endrin (3.3 D), chlorpyrifos (3.2 D), diazinon (2.9 D), BDE 47 (2.7 D), oxadiazon (2.7 D), BDE 85 (2.7 D),  $\alpha$ -endosulfan (2.6 D), and tonalide (2.5 D). (Fig. S5 in the supporting information). A good agreement between the predicted concentrations ( $C_g$  and  $F$ ) and the measured values in the literature for tributylphosphate, BDE 47, and BDE 85 (Fig. 1) indicates that molecular polarity does not have a significant influence on the predicted concentration distribution of polar compounds for a large dataset of indoor environments (e.g., at a nationwide scale). This is due to the fact that other parameters (e.g.,  $C_d$  and  $TSP$ ) used as inputs for the prediction can vary by orders of magnitude among different environments.

### 3.3. Influence of physical parameters on the partitioning of indoor SVOCs

#### 3.3.1. Molar masses and boiling points

The influence of the SVOC molar mass on the partitioning of SVOCs between the gas phase and airborne particles was observed by Takeuchi et al. when studying the  $C_g$  and  $F$  of 34 SVOCs in 6 houses in Japan (Takeuchi et al., 2014).  $p_L^0$  and  $K_{oa}$  can also influence  $K_p$  and  $K_d$ , thereby influencing the partitioning of indoor SVOCs among the different phases. The theoretical relationship between  $K_p$ ,  $p_L^0$ , and the molar mass was addressed as (Pankow, 1994)

$$K_p = \frac{f_{om}RT}{M_{om}\alpha p_{L,T}^0 10^6} \quad (5)$$

where  $f_{om}$  is the weight fraction of the airborne particles absorbing organic materials,  $M_{om}$  (g/mol) is the mean molecular weight of the absorbing organic material,  $\alpha$  is the activity

coefficient of the compound in the organic material phase, and  $p_{L,T}^0$  (Pa) is the saturation vapor pressure of the pure subcooled liquid compound at temperature  $T$ .

The SVOC vapor pressure depends on the temperature, which can be addressed by the Clausius-Clapeyron relationship

$$\ln \frac{p}{p_b} = -\frac{\Delta H_b^v}{R} \left( \frac{1}{T} - \frac{1}{T_b} \right) \quad (6)$$

where  $T_b$  (K) is the normal boiling point of the SVOC,  $p_b$  is the SVOC vapor pressure at its boiling point, and  $\Delta H_b^v$  (J/mol) is the enthalpy of vaporization at the boiling point.

Trouton's rule states that the entropy of vaporization of non-hydrogen-bonded compounds at the normal boiling point is nearly a constant, which can be described by (Mackay et al., 1982)

$$\frac{\Delta H_b^v}{T_b} = \beta + R \ln T_b \quad (7)$$

where  $\beta$  is a regression constant.

Combining Eqs. (6) and (7) yields (Mackay et al., 1982)

$$\ln \frac{p}{p_b} = \left( \frac{\beta}{R} + \ln T_b \right) \left( 1 - \frac{T_b}{T} \right) \quad (8)$$

After replacing  $p_{L,T}^0$  with Eq. (8), Eq. (5) becomes

$$K_p = \frac{f_{om}RT}{10^6 M_{om} \alpha p_b T_b^{(1-\frac{T_b}{T})} e^{\frac{\beta}{R}(1-\frac{T_b}{T})}} \quad (9)$$

Combining Eqs. (1) and (9), the partitioning of SVOCs between the gas phase and airborne particles can be described by

$$\frac{C_g \times TSP}{F} = \frac{1}{K_p} = \frac{AM_{om}T_b^{(1-\frac{T_b}{T})}e^{\frac{BT_b}{T}}}{T} \quad (10)$$

where the constant  $A$  equals  $\frac{10^6 \alpha p_b e^{\frac{\beta}{R}}}{f_{om}R}$  and the constant  $B$  equals  $-\frac{\beta}{R}$ . The constants  $A$  and  $B$  were determined from regressions of the median SVOC concentrations in the gas and particulate phases in the 3.6 million French dwellings using Eq. (10). The  $R^2$  values of the regressions ranged between 0.78 (pesticides) and 0.99 (PAHs) (Table 2). The impact of the molar mass and boiling point of the SVOCs on the SVOC partitioning between the gas phase and airborne particles differed from one chemical family to another probably because of the difference in structure between the chemical families. Notably, the pesticides in the present study were not of the same chemical family, but their values were fitted into a single regression because of the diversity of their families and the limited number of data available within each pesticide family.

<p>Table 2. Relationship of the molar mass and boiling point with the SVOC partitioning between the gas phase and airborne particles</p>
--

We assumed that  $K_d$  can be described by Eq. (10). Therefore, constants  $A$  and  $B$  were determined from the regression of the median SVOC concentrations in both the gas phase and settled dust in the 3.6 million French dwellings according to Eq. (2). The  $R^2$  value associated with the regressions ranged between 0.48 (pesticides) and 0.99 (PAHs) (Table 3). The  $R^2$  values of the regressions of the SVOC partitioning in the gas phase and settled dust were generally lower than those found

between the gas- and particulate-phase SVOC concentrations. This result may be explained by the following reasons. First, the morphology of the settled dust, e.g., size and substrate, differs from that of airborne particles. Second, the direct mass transfer of SVOCs from materials to settled dust may occur (Rauert and Harrad, 2015; Takigami et al., 2008), thereby influencing the partitioning of SVOCs between the gas phase and settled dust (Schripp et al., 2010). As a result, the nature of  $K_d$  may differ from that of  $K_p$ . Therefore, a bias may exist when using Eq. (10) to address  $K_d$ . To better understand the impact of the molar mass and boiling point on the partitioning of SVOCs between the gas phase and settled dust, the partitioning mechanism should be investigated in future studies. Nevertheless, the empirical equations describing the relationship of the molar mass and boiling point with the partitioning of SVOCs among the gas phase, airborne particles and settled dust may lead to a quick prediction of SVOC partitioning among these three phases.

<p>Table 3. Relationship of the molar mass and boiling point with the SVOC partitioning between the gas phase and settled dust</p>
--

### 3.3.2. Saturation vapor pressures and octanol/air partition coefficients

The gas-to-air and air-to-settled dust concentration ratios were compared with the  $p_L^0$  and  $K_{oa}$  of each SVOC. The  $p_L^0$  and  $K_{oa}$  values were the median of numerous estimates in the literature (Wei et al., 2016a). SVOCs with a high  $p_L^0$ , namely, with high volatility, tended to be predominantly found in the gas phase (Fig. S6 in the supporting information). When the  $p_L^0$  at 25 °C was higher than  $6.16 \times 10^{-4}$  Pa, more than 90% of the mass of the SVOCs in indoor air existed in the gas phase. In contrast, when the  $p_L^0$  at 25 °C was lower than  $4.53 \times 10^{-6}$  Pa, more than 90% of the mass of the SVOCs in indoor air existed in the airborne particles. The air-to-settled dust concentration ratio

generally increased as  $p_L^0$  increased. No influence of the  $p_L^0$  on the partitioning of SVOCs between the particulate phase and settled dust was observed.

Since  $K_{oa}$  is related to  $p_L^0$ , the SVOCs with high  $K_{oa}$  tended to be predominantly found in the particulate phase (Fig. S7 in the supporting information). When the  $K_{oa}$  was higher than  $5.07 \times 10^{11}$  at 25 °C, more than 90% of the mass of the SVOCs in indoor air was associated with the particulate phase. When the  $K_{oa}$  was lower than  $2.26 \times 10^9$  at 25 °C, more than 90% of the mass of the SVOCs in indoor air was found in the gas phase. The air-to-dust concentration ratio generally decreased as  $K_{oa}$  increased. No influence of  $K_{oa}$  on the partitioning of SVOCs between the airborne particles and settled dust was observed. A similar observation of the impact of  $K_{oa}$  on the partitioning of SVOCs between the air and settled dust was reported by Dodson et al. when measuring the concentrations of 40 SVOCs in 50 nonsmoker homes in California (Dodson et al., 2015).

The prediction of the  $C_g$  and  $F$  of SVOCs from  $C_d$  in the present study used the distributions of  $p_L^0$  and  $K_{oa}$  to calculate the distributions of  $K_p$  and  $K_d$  (Wei et al., 2016a). Therefore, the observation of the influence of  $p_L^0$  and  $K_{oa}$  on the partitioning of SVOCs among the different phases was not an independent study. Nevertheless, their influences have been addressed in other studies in the literature (Pankow, 1994; Weschler and Nazaroff, 2010).

#### 4. CONCLUSIONS

A probabilistic method based on SVOC partitioning theory and performed through Monte Carlo simulation was used to predict the SVOC concentrations in both the gas and particulate phases from their measured concentrations in settled dust at the nationwide scale in France. The SVOCs

with the highest predicted concentrations in the indoor air were generally phthalates due to their high concentrations in the settled dust and PAHs due to their low  $K_{oa}$  values compared to the other compounds. The SVOCs with the lowest predicted concentrations in the gas phase and airborne particles were generally PBDEs and PCBs due to their low concentrations in the settled dust. These results highlight the importance of considering the different phases for each SVOC to assess different exposure pathways.

The impacts of four physical parameters, i.e., the molar mass, boiling point, saturation vapor pressure and octanol/air partition coefficient, of SVOCs on the partitioning of SVOCs among the different phases was analyzed quantitatively. The analysis revealed that the SVOC partitioning is highly related to the four parameters. Empirical equations were developed to address the relationships among the molar mass, the boiling point, and the concentration ratio of SVOCs among the different phases.

The performance of the model was validated for a large number of phthalates, PCBs and PBDEs, for which measured concentrations in both settled dust, gas and particulate phases were available. There is still a need of data for other SVOCs, such as pesticides, to better assess the performance of the model.

## ACKNOWLEDGMENTS

This work is a part of the ECOS project supported by the French scientific program on endocrine disruptors (PNRPE; Grant n°2100522667); the French Agency for Food, Environmental and Occupational Health and Safety (ANSES; Grant n°2011-1-128); the French Observatory of indoor

air quality (OQAI; Grants 2011 and 2012); the Scientific and Technical Building Centre (CSTB); and the School of Public Health (EHESP). This research received funding from the People Program (Marie Curie Actions) of the European Union Seventh Framework Programme (FP7/2007-2013) under REA grant agreement n. PCOFUND-GA-2013- 609102, through the PRESTIGE Program coordinated by Campus France (PRESTIGE-2015-3-0016).

## REFERENCES

- Batterman, S.A., Chernyak, S., Jia, C., Godwin, C., Charles, S., 2009. Concentrations and emissions of polybrominated diphenyl ethers from U.S. houses and garages. *Environ. Sci. Technol.* doi:10.1021/es8029957
- Bekö, G., Weschler, C.J., Langer, S., Callesen, M., Toftum, J., Clausen, G., 2013. Children's phthalate intakes and resultant cumulative exposures estimated from urine compared with estimates from dust ingestion, inhalation and dermal absorption in their homes and daycare centers. *PLoS One.* doi:10.1371/journal.pone.0062442
- Blanchard, O., Glorennec, P., Mercier, F., Bonvallot, N., Chevrier, C., Ramalho, O., Mandin, C., Bot, B. Le, 2014. Semivolatile organic compounds in indoor air and settled dust in 30 French dwellings. *Environ. Sci. Technol.* doi:10.1021/es405269q
- Brown, T., Dassonville, C., Derbez, M., Ramalho, O., Kirchner, S., Crump, D., Mandin, C., 2015. Relationships between socioeconomic and lifestyle factors and indoor air quality in French dwellings. *Environ. Res.* doi:10.1016/j.envres.2015.04.012

- Degrendele, C., Okonski, K., Melymuk, L., Landlová, L., Kukučka, P., Audy, O., Kohoutek, J., Čupr, P., Klánová, J., 2016. Pesticides in the atmosphere: A comparison of gas-particle partitioning and particle size distribution of legacy and current-use pesticides. *Atmos. Chem. Phys.* 16, 1531–1544. doi:10.5194/acp-16-1531-2016
- Dodson, R.E., Camann, D.E., Morello-Frosch, R., Brody, J.G., Rudel, R.A., 2015. Semivolatile organic compounds in homes: Strategies for efficient and systematic exposure measurement based on empirical and theoretical factors. *Environ. Sci. Technol.* doi:10.1021/es502988r
- Langer, S., Ramalho, O., Derbez, M., Ribéron, J., Kirchner, S., Mandin, C., 2016. Indoor environmental quality in French dwellings and building characteristics. *Atmos. Environ.* 128, 82–91. doi:10.1016/j.atmosenv.2015.12.060
- Liu, C., Morrison, G.C., Zhang, Y., 2012. Role of aerosols in enhancing SVOC flux between air and indoor surfaces and its influence on exposure. *Atmos. Environ.* 55, 347–356. doi:10.1016/j.atmosenv.2012.03.030
- Lohmann, R., Lammel, G., 2004. Adsorptive and absorptive contributions to the gas-particle partitioning of polycyclic aromatic hydrocarbons: State of knowledge and recommended parametrization for modeling. *Environ. Sci. Technol.* 38, 3793–3803. doi:10.1021/es035337q
- Mackay, D., Bobra, A., Chan, D.W., Shiu, W.Y., 1982. Vapor Pressure Correlations for Low-Volatility Environmental Chemicals. *Environ. Sci. Technol.* doi:10.1021/es00104a004
- Mandin, C., Mercier, F., Lucas, J.-P., Ramalho, O., Blanchard, O., Bonvallot, N., Raffy, G., Gilles, E., Gloennec, P., Le Bot, B., 2013. Semi-volatile organic compounds in home

- settled dust: a nationwide survey in France, in: Conference on Environment and Health, 19–23 August 2013, Basel, Switzerland. doi:<http://dx.doi.org/10.1289/ehp.ehbase113>
- Mandin, C., Mercier, F., Ramalho, O., Lucas, J.P., Gilles, E., Blanchard, O., Bonvallot, N., Glorennec, P., Le Bot, B., 2016. Semi-volatile organic compounds in the particulate phase in dwellings: A nationwide survey in France. *Atmos. Environ.* doi:10.1016/j.atmosenv.2016.04.016
- Pankow, J.F., 1994. An absorption model of gas/particle partitioning of organic compounds in the atmosphere. *Atmos. Environ.* doi:10.1016/1352-2310(94)90093-0
- Pelletier, M., Bonvallot, N., Ramalho, O., Mandin, C., Wei, W., Raffy, G., Mercier, F., Blanchard, O., Le Bot, B., Glorennec, P., 2017. Indoor residential exposure to semivolatile organic compounds in France. *Environ. Int.* 109, 81–88. doi:10.1016/j.envint.2017.08.024
- Rauert, C., Harrad, S., 2015. Mass transfer of PBDEs from plastic TV casing to indoor dust via three migration pathways — A test chamber investigation. *Sci. Total Environ.* 536, 568–574. doi:<https://doi.org/10.1016/j.scitotenv.2015.07.050>
- Schripp, T., Fauck, C., Salthammer, T., 2010. Chamber studies on mass-transfer of di(2-ethylhexyl)phthalate (DEHP) and di-n-butylphthalate (DnBP) from emission sources into house dust. *Atmos. Environ.* doi:10.1016/j.atmosenv.2010.04.054
- Shi, S., Zhao, B., 2012. Comparison of the predicted concentration of outdoor originated indoor polycyclic aromatic hydrocarbons between a kinetic partition model and a linear instantaneous model for gas-particle partition. *Atmos. Environ.* doi:10.1016/j.atmosenv.2012.05.007

- Takeuchi, S., Kojima, H., Saito, I., Jin, K., Kobayashi, S., Tanaka-Kagawa, T., Jinno, H., 2014. Detection of 34 plasticizers and 25 flame retardants in indoor air from houses in Sapporo, Japan. *Sci. Total Environ.* doi:10.1016/j.scitotenv.2014.04.011
- Takigami, H., Suzuki, G., Hirai, Y., Sakai, S. ichi, 2008. Transfer of brominated flame retardants from components into dust inside television cabinets. *Chemosphere* 73, 161–169. doi:10.1016/j.chemosphere.2008.06.032
- Venier, M., Audy, O., Vojta, Š., Bečanová, J., Romanak, K., Melymuk, L., Krátká, M., Kukučka, P., Okeme, J., Saini, A., Diamond, M.L., Klánová, J., 2016. Brominated flame retardants in the indoor environment - Comparative study of indoor contamination from three countries. *Environ. Int.* 94, 150–160. doi:10.1016/j.envint.2016.04.029
- Vykoukalová, M., Venier, M., Vojta, Š., Melymuk, L., Bečanová, J., Romanak, K., Prokeš, R., Okeme, J.O., Saini, A., Diamond, M.L., Klánová, J., 2017. Organophosphate esters flame retardants in the indoor environment. *Environ. Int.* 106, 97–104. doi:10.1016/j.envint.2017.05.020
- Webster, T.F., Harrad, S., Millette, J.R., Holbrook, R.D., Davis, J.M., Stapleton, H.M., Allen, J.G., McClean, M.D., Ibarra, C., Abdallah, M.A.E., Covaci, A., 2009. Identifying transfer mechanisms and sources of decabromodiphenyl ether (BDE 209) in indoor environments using environmental forensic microscopy. *Environ. Sci. Technol.* doi:10.1021/es803139w
- Wei, W., Mandin, C., Blanchard, O., Mercier, F., Pelletier, M., Le Bot, B., Glorennec, P., Ramalho, O., 2017a. Predicting the gas-phase concentration of semi-volatile organic compounds from airborne particles: Application to a French nationwide survey. *Sci. Total*

Environ. 576, 319–325. doi:10.1016/j.scitotenv.2016.10.074

- Wei, W., Mandin, C., Blanchard, O., Mercier, F., Pelletier, M., Le Bot, B., Glorennec, P., Ramalho, O., 2016a. Distributions of the particle/gas and dust/gas partition coefficients for seventy-two semi-volatile organic compounds in indoor environment. *Chemosphere* 153, 212–219. doi:10.1016/j.chemosphere.2016.03.007
- Wei, W., Mandin, C., Blanchard, O., Mercier, F., Pelletier, M., Le Bot, B., Glorennec, P., Ramalho, O., 2016b. Temperature dependence of the particle/gas partition coefficient: An application to predict indoor gas-phase concentrations of semi-volatile organic compounds. *Sci. Total Environ.* 563–564, 506–512. doi:10.1016/j.scitotenv.2016.04.106
- Wei, W., Mandin, C., Ramalho, O., 2017b. Reactivity of semivolatile organic compounds with hydroxyl radicals, nitrate radicals, and ozone in indoor air. *Int. J. Chem. Kinet.* 49, 506–521.
- Weschler, C.J., Nazaroff, W.W., 2017. Growth of organic films on indoor surfaces. *Indoor Air* 27, 1101–1112. doi:10.1111/ina.12396
- Weschler, C.J., Nazaroff, W.W., 2010. SVOC partitioning between the gas phase and settled dust indoors. *Atmos. Environ.* doi:10.1016/j.atmosenv.2010.06.029
- Weschler, C.J., Nazaroff, W.W., 2008. Semivolatile organic compounds in indoor environments. *Atmos. Environ.* doi:10.1016/j.atmosenv.2008.09.052
- Wu, Y., Eichler, C., Cao, J., Benning, J., Olson, A., Chen, S., Liu, C., Vejerano, E., Marr, L., Little, J., 2018. Particle/gas partitioning of phthalates to organic and inorganic airborne

particles in the indoor environment. *Environ. Sci. Technol.* 52, 3583–3590.

Xu, Y., Cohen Hubal, E.A., Little, J.C., 2010. Predicting residential exposure to phthalate plasticizer emitted from vinyl flooring: Sensitivity, uncertainty, and implications for biomonitoring. *Environ. Health Perspect.* 118, 253–258. doi:10.1289/ehp.0900559

Xu, Y., Liu, Z., Park, J., Clausen, P.A., Benning, J.L., Little, J.C., 2012. Measuring and predicting the emission rate of phthalate plasticizer from vinyl flooring in a specially-designed chamber. *Environ. Sci. Technol.* 46, 12534–12541. doi:10.1021/es302319m

Zhang, X., Diamond, M.L., Robson, M., Harrad, S., 2011. Sources, Emissions, and Fate of Polybrominated Diphenyl Ethers and Polychlorinated Biphenyls Indoors in Toronto, Canada. *Environ. Sci. Technol.* 45, 3268–3274. doi:10.1021/es102767g

## Tables

Table 1. SVOC concentrations in the gas phase ( $C_g$ ) and airborne particles ( $F$ )

Pollutant	$C_g$ (pg/m <sup>3</sup> )			$F$ (pg/m <sup>3</sup> )		
	P25	P50	P75	P25	P50	P75
BBP	$8.7 \times 10^2$	$7.8 \times 10^3$	$8.0 \times 10^4$	$9.5 \times 10^1$	$1.3 \times 10^3$	$2.4 \times 10^4$
DBP	$3.4 \times 10^4$	$9.7 \times 10^4$	$2.8 \times 10^5$	$7.4 \times 10^2$	$3.3 \times 10^3$	$1.5 \times 10^4$
DiBP	$1.0 \times 10^5$	$2.7 \times 10^5$	$8.5 \times 10^5$	$4.9 \times 10^2$	$3.3 \times 10^3$	$2.2 \times 10^4$
DEP	$2.2 \times 10^4$	$3.2 \times 10^5$	$1.3 \times 10^6$	$5.6 \times 10^2$	$2.2 \times 10^3$	$8.9 \times 10^3$
DEHP	$5.0 \times 10^2$	$2.7 \times 10^3$	$1.5 \times 10^4$	$3.7 \times 10^2$	$5.7 \times 10^3$	$1.3 \times 10^5$
DiNP	$4.3 \times 10^1$	$1.8 \times 10^2$	$7.9 \times 10^2$	$5.4 \times 10^1$	$4.7 \times 10^2$	$4.7 \times 10^3$
BDE28	$3.0 \times 10^0$	$7.1 \times 10^0$	$1.3 \times 10^1$	$3.4 \times 10^{-1}$	$1.0 \times 10^0$	$3.8 \times 10^0$
BDE47	$2.1 \times 10^0$	$5.5 \times 10^0$	$1.4 \times 10^1$	$1.4 \times 10^0$	$6.0 \times 10^0$	$2.9 \times 10^1$
BDE85	$2.0 \times 10^{-2}$	$5.7 \times 10^{-2}$	$1.4 \times 10^{-1}$	$7.7 \times 10^{-2}$	$4.3 \times 10^{-1}$	$2.2 \times 10^0$
BDE99	$2.3 \times 10^{-1}$	$6.7 \times 10^{-1}$	$1.9 \times 10^0$	$3.3 \times 10^{-1}$	$2.2 \times 10^0$	$1.7 \times 10^1$
BDE100	$5.2 \times 10^{-2}$	$1.8 \times 10^{-1}$	$8.8 \times 10^{-1}$	$1.6 \times 10^{-1}$	$1.1 \times 10^0$	$2.0 \times 10^1$
BDE119	$1.6 \times 10^{-2}$	$4.2 \times 10^{-2}$	$1.0 \times 10^{-1}$	$4.0 \times 10^{-2}$	$2.3 \times 10^{-1}$	$1.3 \times 10^0$
BDE153	$1.1 \times 10^{-2}$	$3.9 \times 10^{-2}$	$1.3 \times 10^{-1}$	$1.8 \times 10^{-1}$	$2.0 \times 10^0$	$2.3 \times 10^1$
BDE154	$1.4 \times 10^{-2}$	$5.3 \times 10^{-2}$	$2.0 \times 10^{-1}$	$8.4 \times 10^{-2}$	$8.8 \times 10^{-1}$	$8.4 \times 10^0$
BDE209	$1.2 \times 10^{-6}$	$8.2 \times 10^{-6}$	$8.9 \times 10^{-5}$	$1.3 \times 10^{-3}$	$5.1 \times 10^{-2}$	$3.0 \times 10^0$
PCB28	$7.9 \times 10^1$	$2.0 \times 10^2$	$6.7 \times 10^2$	$5.0 \times 10^{-1}$	$2.6 \times 10^0$	$1.2 \times 10^1$
PCB31	$9.6 \times 10^1$	$2.2 \times 10^2$	$6.4 \times 10^2$	$5.5 \times 10^{-1}$	$2.5 \times 10^0$	$1.3 \times 10^1$
PCB52	$6.1 \times 10^1$	$1.7 \times 10^2$	$1.1 \times 10^3$	$1.4 \times 10^0$	$6.5 \times 10^0$	$5.3 \times 10^1$

PCB77	$1.5 \times 10^0$	$4.9 \times 10^0$	$1.8 \times 10^1$	$7.3 \times 10^{-2}$	$3.7 \times 10^{-1}$	$1.9 \times 10^0$
PCB101	$1.5 \times 10^1$	$6.3 \times 10^1$	$5.6 \times 10^2$	$7.5 \times 10^{-1}$	$6.2 \times 10^0$	$6.1 \times 10^1$
PCB105	$2.5 \times 10^0$	$8.1 \times 10^0$	$5.5 \times 10^1$	$3.1 \times 10^{-1}$	$1.8 \times 10^0$	$1.8 \times 10^1$
PCB118	$4.1 \times 10^0$	$1.8 \times 10^1$	$1.7 \times 10^2$	$3.8 \times 10^{-1}$	$3.2 \times 10^0$	$3.6 \times 10^1$
PCB126	$3.5 \times 10^{-1}$	$1.1 \times 10^0$	$3.0 \times 10^0$	$4.4 \times 10^{-2}$	$2.0 \times 10^{-1}$	$8.9 \times 10^{-1}$
PCB138	$2.3 \times 10^0$	$9.8 \times 10^0$	$9.4 \times 10^1$	$4.7 \times 10^{-1}$	$3.8 \times 10^0$	$4.0 \times 10^1$
PCB153	$1.4 \times 10^0$	$7.2 \times 10^0$	$7.0 \times 10^1$	$4.0 \times 10^{-1}$	$3.7 \times 10^0$	$4.2 \times 10^1$
4,4'DDE	$7.7 \times 10^0$	$2.9 \times 10^1$	$1.2 \times 10^2$	$2.1 \times 10^{-1}$	$1.1 \times 10^0$	$5.5 \times 10^0$
$\gamma$ -HCH	$3.0 \times 10^2$	$2.4 \times 10^3$	$1.8 \times 10^4$	$1.0 \times 10^0$	$1.1 \times 10^1$	$1.2 \times 10^2$
Aldrin	$2.0 \times 10^1$	$4.2 \times 10^2$	$1.1 \times 10^4$	$1.6 \times 10^{-1}$	$7.1 \times 10^0$	$3.3 \times 10^2$
Dieldrin	$1.1 \times 10^1$	$5.2 \times 10^1$	$2.3 \times 10^2$	$4.1 \times 10^{-1}$	$3.0 \times 10^0$	$2.2 \times 10^1$
Endrin	$1.7 \times 10^1$	$8.3 \times 10^1$	$3.8 \times 10^2$	$8.2 \times 10^{-1}$	$6.6 \times 10^0$	$5.1 \times 10^1$
Oxadiazon	$8.3 \times 10^{-1}$	$2.4 \times 10^0$	$9.4 \times 10^0$	$5.3 \times 10^{-1}$	$2.8 \times 10^0$	$1.4 \times 10^1$
$\alpha$ -Endosulfan	$9.3 \times 10^1$	$1.0 \times 10^3$	$1.2 \times 10^4$	$5.5 \times 10^0$	$9.5 \times 10^1$	$2.0 \times 10^3$
Permethrin	$1.6 \times 10^1$	$8.8 \times 10^1$	$5.2 \times 10^2$	$2.9 \times 10^1$	$2.5 \times 10^2$	$2.5 \times 10^3$
Cyfluthrin	$9.0 \times 10^{-2}$	$5.4 \times 10^{-1}$	$3.8 \times 10^0$	$4.9 \times 10^{-1}$	$6.4 \times 10^0$	$1.2 \times 10^2$
Cypermethrin	$1.7 \times 10^{-1}$	$1.4 \times 10^0$	$2.3 \times 10^1$	$9.9 \times 10^{-1}$	$1.8 \times 10^1$	$4.2 \times 10^2$
Deltamethrin	$2.5 \times 10^{-1}$	$1.7 \times 10^0$	$1.1 \times 10^1$	$2.1 \times 10^0$	$2.3 \times 10^1$	$3.4 \times 10^2$
Chlorpyrifos	$2.9 \times 10^1$	$1.1 \times 10^2$	$4.4 \times 10^2$	$1.0 \times 10^0$	$5.3 \times 10^0$	$2.9 \times 10^1$
Diazinon	$5.8 \times 10^0$	$1.3 \times 10^1$	$3.6 \times 10^1$	$1.6 \times 10^{-1}$	$7.4 \times 10^{-1}$	$3.1 \times 10^0$
Dichlorvos	$1.4 \times 10^4$	$4.0 \times 10^4$	$1.1 \times 10^5$	$7.7 \times 10^{-1}$	$3.6 \times 10^0$	$1.6 \times 10^1$
Anthracene	$6.9 \times 10^3$	$1.8 \times 10^4$	$4.5 \times 10^4$	$3.4 \times 10^1$	$2.3 \times 10^2$	$2.0 \times 10^3$
Fluorene	$3.7 \times 10^4$	$6.6 \times 10^4$	$1.2 \times 10^5$	$2.8 \times 10^1$	$1.0 \times 10^2$	$3.9 \times 10^2$

Phenanthrene	$5.0 \times 10^4$	$9.4 \times 10^4$	$2.1 \times 10^5$	$1.9 \times 10^2$	$9.2 \times 10^2$	$6.3 \times 10^3$
Benzo[a]pyrene	$8.2 \times 10^0$	$4.6 \times 10^1$	$2.5 \times 10^2$	$6.8 \times 10^0$	$1.9 \times 10^2$	$5.4 \times 10^3$
Acenaphthene	$1.5 \times 10^4$	$3.5 \times 10^4$	$8.4 \times 10^4$	$6.2 \times 10^0$	$2.5 \times 10^1$	$1.1 \times 10^2$
Galaxolide	$1.4 \times 10^4$	$3.2 \times 10^4$	$7.0 \times 10^4$	$7.1 \times 10^1$	$2.6 \times 10^2$	$9.6 \times 10^2$
Tonalide	$2.7 \times 10^3$	$8.4 \times 10^3$	$2.7 \times 10^4$	$1.7 \times 10^1$	$7.4 \times 10^1$	$3.3 \times 10^2$
Tributylphosphate	$1.1 \times 10^4$	$2.1 \times 10^4$	$4.3 \times 10^4$	$9.2 \times 10^0$	$3.2 \times 10^1$	$1.2 \times 10^2$
Bisphenol A	$3.0 \times 10^0$	$7.8 \times 10^0$	$2.1 \times 10^1$	$2.3 \times 10^0$	$1.9 \times 10^1$	$1.9 \times 10^2$

Table 2. Relationship of the molar mass and boiling point with the SVOC partitioning between the gas phase and airborne particles

SVOCs	<i>A</i>	<i>B</i>	<i>R</i> <sup>2</sup>
Phthalates	4.67×10 <sup>11</sup>	-6.35	0.85
PBDEs	1.43×10 <sup>13</sup>	-8.21	0.92
PCBs	4.95×10 <sup>18</sup>	-10.35	0.91
Pesticides	2.17×10 <sup>14</sup>	-8.98	0.78
PAHs	3.45×10 <sup>14</sup>	-8.98	0.99
All the SVOCs	6.78×10 <sup>14</sup>	-9.55	0.83

$$\frac{C_g \times TSP}{F} = \frac{AM_{om}T_b \left(1 - \frac{T_b}{T}\right)^{\frac{B}{T}} e^{\frac{A}{T}}}{T}. C_g \text{ and } F \text{ have units of } \text{pg/m}^3; TSP \text{ has a unit of } \mu\text{g/m}^3.$$

Table 3. Relationship between the molar mass and boiling point, and SVOC partitioning in the gas phase and settled dust

SVOCs	<i>A</i>	<i>B</i>	<i>R</i> <sup>2</sup>
Phthalates	4.19×10 <sup>17</sup>	-15.41	0.90
PBDEs	4.40×10 <sup>23</sup>	-20.48	0.97
PCBs	3.23×10 <sup>23</sup>	-20.34	0.74
Pesticides	8.39×10 <sup>12</sup>	-9.10	0.48
PAHs	1.49×10 <sup>14</sup>	-9.72	0.99
All the SVOCs	2.28×10 <sup>17</sup>	-14.18	0.64

$$\frac{C_g}{C_d} = \frac{AM_{om}T_b \left(1 - \frac{T_b}{T}\right)^{\frac{BT_b}{T}}}{T}. C_g \text{ and } C_d \text{ have units of } \text{pg/m}^3 \text{ and } \text{ng/g}, \text{ respectively.}$$

**HIGHLIGHTS**

- ▶ The concentrations of 48 SVOCs in indoor gas and particle phases were predicted.
- ▶ The concentration distributions for 3.6 million dwellings in France were obtained.
- ▶ The probabilistic approach was based on Monte Carlo simulation.
- ▶ The partition coefficient can be estimated from the molar mass and boiling point.

ACCEPTED MANUSCRIPT

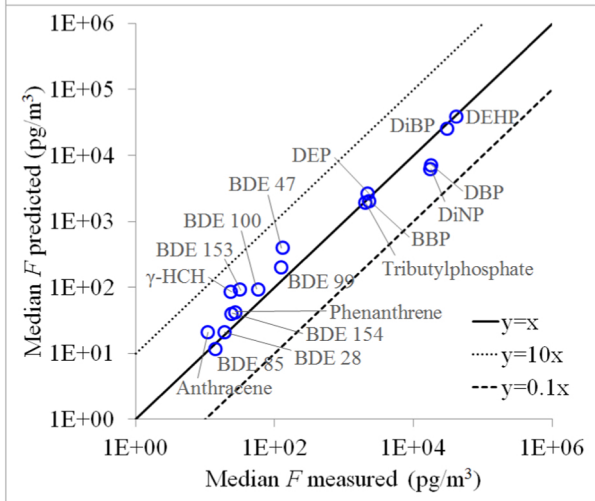
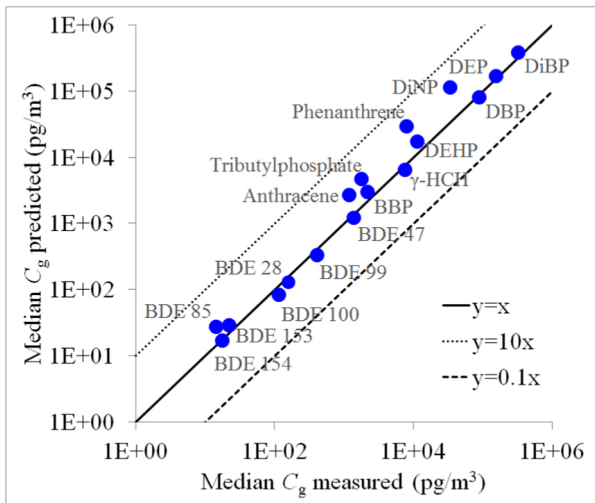


Figure 1

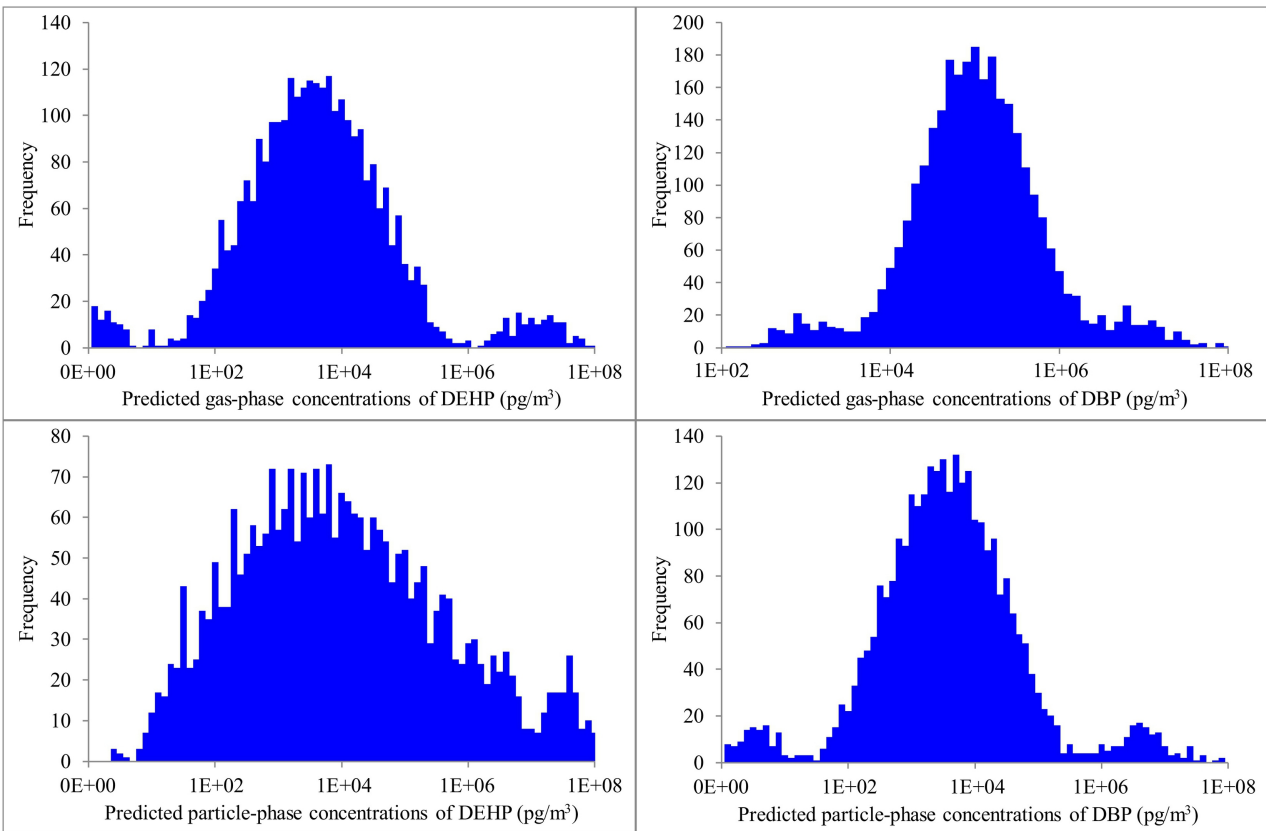


Figure 2

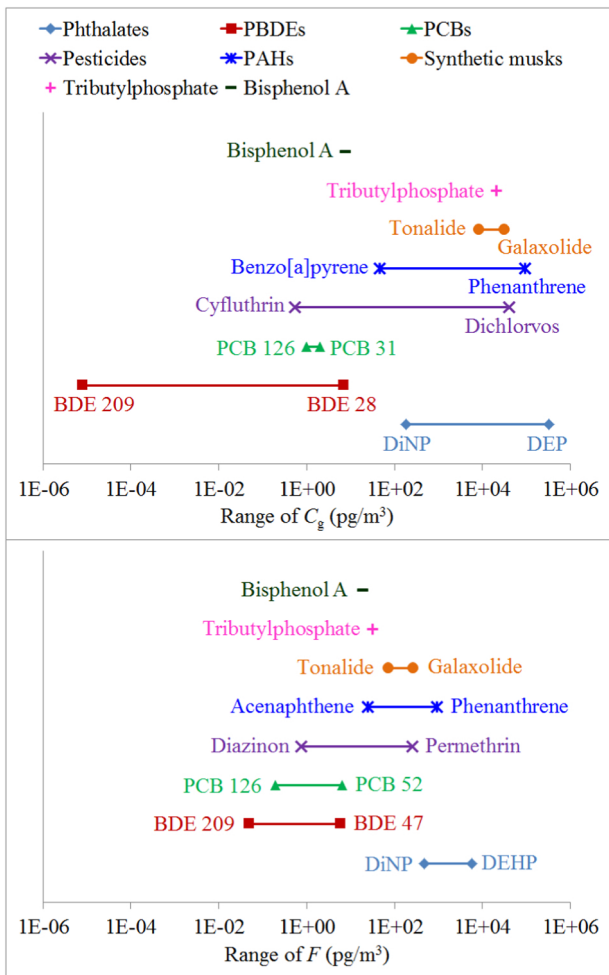


Figure 3

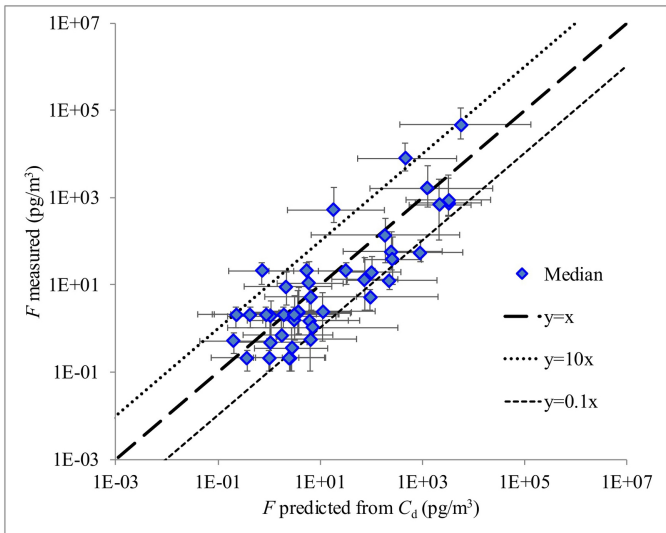


Figure 4

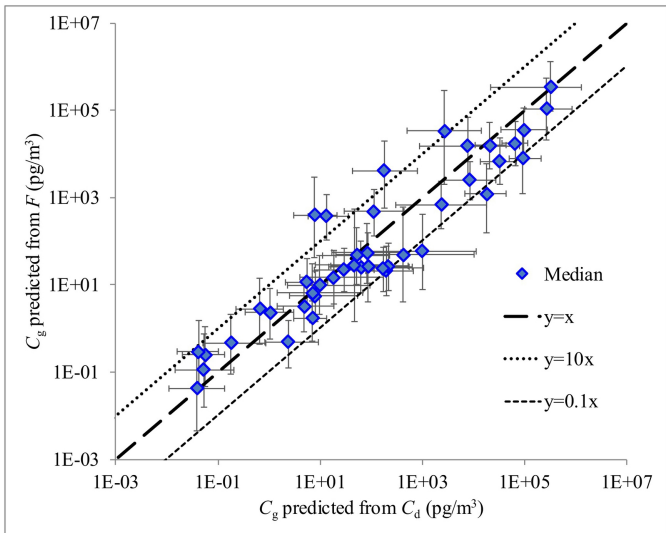


Figure 5